

# Leaching of a low-grade, copper-nickel sulfide ore. 1. Key parameters impacting on Cu recovery during column bioleaching

H.R. Watling<sup>1\*</sup>, A.D. Elliot,<sup>1</sup> M. Maley,<sup>2</sup> W. van Bronswijk<sup>2</sup> and C. Hunter<sup>3</sup>

<sup>1</sup> AJ Parker Cooperative Research Centre for Integrated Hydrometallurgy Solutions, CSIRO Minerals, PO Box 7229, Karawara, Western Australia 6152

<sup>2</sup> Department of Applied Chemistry, Curtin University of Technology, GPO Box U1987, Perth, Western Australia 6845

<sup>3</sup> Pacific Ore Technology, PO Box 1073, West Perth, Western Australia 6872

\*For correspondence email [Helen.Watling@csiro.au](mailto:Helen.Watling@csiro.au) , Tel: +61 8 9334 8034, Fax: +61 8 9334 8001

## Abstract

This study was prompted by the disparate recoveries of nickel (>70%) and copper (<20%) from a test heap of copper-nickel sulfide ore after about 200 days of leaching. Variables tested in bioleaching columns charged with a pyrrhotite-rich, chalcopyrite and pentlandite ore were acid pre-conditioning, inoculation and aeration. The results indicated that the rapid reaction of pyrrhotite with acid created conditions that impacted directly and/or indirectly on copper recovery. Important reactions were hydrogen sulfide formation, high soluble iron concentrations and the formation of large amounts of elemental sulfur. It was hypothesized that copper loss, evidenced by copper re-distribution during passage through the ore, was mainly the result of reaction with hydrogen sulfide to form covellite, although this could not be confirmed by XRD analysis of leached residues. A layer of iron-oxy-hydroxy-sulfate “scale” on particle surfaces encapsulated sulfide grains as well as elemental sulfur formed by the oxidation of pyrrhotite and was of sufficient depth and integrity to have hindered but not prevented leaching and bioleaching. Lack of aeration (oxygen, carbon dioxide) impacted on ferrous ion biooxidation and probably sulfur biooxidation. More extensive sulfur biooxidation to form acid might have lowered the

solution pH and reduced the amount of scale formation, resulting in higher ferric ion concentrations and better chalcopyrite oxidation.

Keywords: Chalcopyrite; Pentlandite; Pyrrhotite; Leaching; Bioleaching

## 1. Introduction

The economic extraction of metals from low-grade ores requires low-cost processing methods such as dump and heap leaching. The most successful heap leaching operations have been those processing copper oxides and secondary copper sulfide minerals such as chalcocite. Together with dump leaching of mine waste, heap leaching contributes about 20% of annual world copper production (Watling, 2006). The leaching of several low-grade nickel sulfide ores has also been investigated in pilot-scale heaps (Watling, 2008), including test heaps at Radio Hill, Western Australia and at Talvivaara, Finland.

The comprehensive studies over three decades on the complex black-schist ore of Talvivaara (Sotkamo, Finland) was driven by the potential of developing a low-cost technology with which to exploit the largest European nickel deposit, some 340Mt of ore with average grades 0.56% Zn, 0.27% Ni, 0.14% Cu and 0.02% Co (Puhakka et al., 2007). It is a pyrrhotite- and pyrite-rich ore in which nickel is distributed between pentlandite, pyrrhotite and pyrite. The Talvivaara test heap exhibited, in common with the Radio Hill test heap, poor copper extraction, only 2% in 500 days compared with a nickel recovery of 92%.

The test heap at Radio Hill was constructed using copper-nickel ore from the Mt Sholl deposit. The results obtained from this test heap prompted the studies described in the present paper and are thus summarised specifically.

### 1.1. Copper-nickel ore test heap

The test heap flow sheet was unusual in that two separate, aerated bio-heaps were operated in parallel (Figure 1). The first heap, five metres high and consisting of 5000 tonnes of crushed ore (100% <7.5 mm), was acid conditioned until the heap discharge was pH <2.2. It was then inoculated with the predominantly sulfur-oxidising mixed microbial culture and allowed to cure. This heap was re-inoculated with the sulfur-oxidising culture

when irrigation was commenced. The second heap of inert rock was also acid conditioned and was inoculated with a mixed culture of ferrous ion oxidising bacteria. This heap assisted in iron control around the circuit.

Temperatures in the sulfide ore heap were monitored via thermocouples placed at different depths during heap construction. Temperatures varied dramatically in a manner related to heap aeration and solution management (Figure 2).

Monitoring began with the acid conditioning and inoculation phase, during which temperatures dropped (Figure 2, A). A marked temperature increase (Figure 2, B) occurred when the irrigation was temporarily shut down but aeration was continued. Temperatures near the top of the heap only began to drop when the irrigation rate was increased from 10 to 30 L/m<sup>2</sup>/h. Heat was carried downwards during this period and bottom temperatures increased accordingly (Figure 2, C). However, the irrigation rate was subsequently lowered to reduce ponding on the heap surface (Figure 2, D). Temperatures thereafter stabilised with time at about 45 °C, possibly due to diminished amounts of reactive sulfides in the partially leached heap.

The test heap of Mt Sholl ore was operated using the BioHeap<sup>TM</sup> technology (Hunter, 2001; 2002), integral to which is a proprietary, moderately thermophilic, mixed culture of predominantly sulfur-oxidising bacteria and archaea (Hunter et al., 2007). The culture assisted the oxidation of both pentlandite and chalcopyrite in the temperature range 40-60 °C and the pH range 0.8-2.2; solution redox potential increased slowly but steadily from about 400 to 460 mV vs Ag/AgCl in 29-day laboratory tests, clearly indicating minimal ferrous ion biooxidation. The inefficient oxidation of ferrous ion by this culture, resulting in leachates with moderately low solution potentials, was expected to enhance the oxidation of chalcopyrite, as reported by Hiroyoshi et al. (2001).

As part of the preliminary test work for the heap, a five metre tall, 150 mm diameter column was charged with 60 kg ore (100% <4.8 mm) which had been wetted and acid conditioned to distribute the fines evenly (agglomeration). Further acid conditioning was achieved by recycling acidified water through the ore until the discharge solution was pH 1.8. The column was heated to 50 °C and was aerated. Inoculation was achieved via the feed solution by substituting 20 L of acidified water with 20 L of bacterial culture. Thus, ore inoculation in the column was a “top-down” process. Column leaching results were encouraging in that about 60% of both nickel and copper were extracted in 60 days (Figure

3). Rates of extraction were very similar to that point with no discernible lag time. Nickel extraction continued to increase to about 70% by 90 days, but little additional copper was extracted in the time frame of the experiment.

In about one year of test heap operation, 90% of the contained nickel and 50% of the contained copper were leached into solution. However, the test heap results differed from the column results in that, while extraction rates for nickel and copper were similar, copper extraction lagged behind nickel extraction by 5-6 months. It was hypothesised that the copper had been leached from the chalcopyrite, as was the case in the tall column, but subsequently re-deposited in the ore bed.

## *1.2. Research strategy*

Precipitation of copper onto sulfide minerals has been reported (Ahonen and Tuovinen, 1994), but not to an extent sufficient to account for the copper recovery that was experienced in the test heap. A lack of oxygen could contribute to the observed copper loss, even though the heap was aerated via perforated pipes located about one metre from its base. Lizama (2001) reported significant oxygen depletion with increasing depth in a chalcocite heap of similar height. Such a decrease in available oxygen could impact on both the bacterial activity and the chemical environment in the heap (du Plessis et al., 2001). In addition, the possibility that low acidity (high leachate pH) also contributed to copper re-deposition could not be ruled out, as pyrrhotite-rich ores are well known acid consumers (Ahonen and Tuovinen, 1994; Belzile et al., 2004).

The reasons for the observed copper re-deposition in the test heap were investigated using copper-nickel sulfide ore obtained from the Mt Sholl deposit. Bioleaching experiments were conducted to determine the key parameters impacting on copper recovery. The mineralogy of the ore and leached residues was examined to assist with results interpretation.

## **2. Materials and Methods**

### *2.1. Copper-nickel sulfide ore*

The mixed sulfide ore consisted of a mainly silicate matrix (~80-90%), with pyrrhotite ( $\text{Fe}_{1-x}\text{S}$ , where  $x$  varies from 0 to 0.125), chalcopyrite ( $\text{CuFeS}_2$ ) and pentlandite ( $(\text{Fe,Ni})_9\text{S}_8$ ). [In this paper the stoichiometry of pyrrhotite is shown as  $\text{FeS}$ .]

As part of the preliminary test work for the trial heap, a sample of the ore was crushed to -6.3 mm and wet screened at 75  $\mu\text{m}$ . The -6.3 +0.075 mm fraction was further screened to yield size fractions -6.3 +2.8, -2.8 +1.18, -1.18 +0.6, -0.6 +0.3, and -0.3 +0.075 mm which were subjected to heavy liquid separation at a density of 2.96  $\text{t/m}^3$  using tetrabromoethane (TBE). The TBE sinks fractions were then subjected to further heavy liquid separation at a density of 3.32  $\text{t/m}^3$  using di-iodomethane. The float and sinks fractions were submitted for elemental analysis.

For the column tests described in this paper, the ore was crushed and the -6.7 +4.75 mm size fraction, between that of the initial tall column (100% <4.8 mm) and the test heap (100% <7.5 mm), was separated by sieving. Representative samples of the ore used in each column were separated from the bulk by riffle splitting and the chemical compositions determined because there was considerable variation in sulfide composition for different drums of ore.

## 2.2. Microbiology

*Sulfobacillus thermosulfidooxidans* (DSM 9293<sup>T</sup>), *Sulfobacillus acidophilus* (DSM 10332<sup>T</sup>), *Acidithiobacillus caldus* DSM 8584<sup>T</sup> and *Acidimicrobium ferrooxidans* DSM 10331<sup>T</sup> were obtained from the German Collection of Microorganisms and Cell Cultures (DSMZ) and grown in individual cultures using their DSM-designated media. Basal salts medium (BSM) was prepared by adding 1.5 g/L  $(\text{NH}_4)_2\text{SO}_4$ , 0.25 g/L  $\text{KH}_2\text{PO}_4$  and 0.25 g/L  $\text{MgSO}_4$  to distilled water, adjusting the pH to 1.8 with concentrated  $\text{H}_2\text{SO}_4$  and sterilizing at 121 °C, 100 kPa for 20 minutes. Each species was subcultured into basal salts medium supplemented with ferrous ions (10 g/L  $\text{FeSO}_4 \cdot 7\text{H}_2\text{O}$ ), sterile elemental sulfur (5 g/L) and yeast extract (0.1 g/L). A mixed bacterial culture containing the four species was then prepared in the growth medium and slowly adapted to growth on the copper-nickel ground ore in an air-lift reactor operated at 45 °C. The resulting mixed culture was used as inoculum for the column experiments.

The number of viable bacteria in column discharge solutions was determined using serial dilution and subsequent incubation on plates prepared with Gel-Rite® gelling agent.

For each sample, plates with ferrous ion growth substrate and with tetrathionate growth substrate were prepared. Plates were incubated at 45 °C for 7 days, after which the number of colonies were counted. Numbers of viable iron- and sulfur-oxidising bacteria were estimated.

### 2.3. *Column bioleaching*

Representative, accurately weighed 10 kg portions of ore were acid conditioned with 900 mL dilute sulfuric acid (pH 1.8) or with water (pH 7) to agglomerate any fine particles. The ore was then loaded into one-metre tall, 150 mm diameter water-jacketed columns equipped with individual 8.5 L solution reservoirs. The columns were heated to 45°C, aerated at 2 L/min, and operated in solution-recycle mode for one week with dilute sulfuric acid (pH 1.8) to dissolve acid-soluble ore components. This simulated the start-up procedure for the test heap in which pond water (pH 1.4-1.8) was recycled through the heap until the discharged solution was pH <2.2, prior to inoculation. The irrigation rate was 1 mL/min. The reservoir solution pH was maintained at pH 1.8 by the addition of concentrated sulfuric acid, as required, for the duration of the experiment. Reservoir solution pH, redox potential, ferrous ion, Ni, Cu and Fe content were monitored periodically for up to 200 days.

For the abiotic columns, a biocide, sodium benzoate, was added to the reservoir solution to a concentration of 0.1 g/L to suppress the growth of any contaminant bacteria in the column or the reservoir. Redox potentials remained below 400 mV (vs Ag/AgCl) throughout the experiment for the leachates of the abiotic columns, suggesting this strategy was successful.

At column termination, leached residues from the columns were rinsed free of leachate using dilute sulfuric acid (pH 1.8) for 3 days, drained overnight, removed from the column and oven-dried at 50°C for 16 hours and stored for further analysis.

### 2.4. *Sample analysis*

Solutions were analysed for Ni, Cu and Fe using a Varian Liberty 220 inductively coupled plasma – atomic emission spectrometer (ICP-AES). The plasma was located in the axial position, with a total sample uptake time of 18 seconds and a washout time of 15

seconds. Solid pulverised ore and leached residue samples were digested in aqua regia and the Ni, Cu and Fe concentrations in digests also determined using ICP-AES.

Ferrous ion concentrations were determined colorimetrically using a procedure adapted from [Wilson \(1960\)](#). A volume of the analyte solution (80  $\mu\text{L}$ ) was added to an ammonium acetate buffer containing 2,2-dipyridyl (4 mL). The absorbance of the resultant pink solution was measured at 525 nm using a Cary 50 Bio UV-vis spectrometer, with the ferrous concentration determined via a previously prepared calibration curve. Where necessary, samples were diluted quantitatively with pH 2 sulfuric acid before addition to the dipyrindyl reagent to give an absorbance within the calibration range.

Representative subsamples of head and residue samples were obtained through riffing of the whole sample. In addition subsamples from column residues were sieved and the fines passing 500  $\mu\text{m}$  were collected. To avoid over-grinding of the samples, comminution of the subsamples was achieved through a combination of sieving through a 212  $\mu\text{m}$  sieve followed by 10 seconds of pulverising of the coarse fraction in a ring mill. This cycle was repeated until the whole sample had passed through the sieve. Pulverised samples were mixed and split for elemental and X-ray diffraction analysis.

For quantitative X-ray diffraction analysis (QXRD), samples were accurately weighed with fluorite (10 wt%) as an internal standard. They were then wet-micronised with ethanol for 15 minutes to minimize oxidation and over-grinding, and then pan dried at room temperature for three days prior to collection and analysis. X-ray powder diffraction patterns were acquired using a Philips X'Pert Automated Powder Diffractometer fitted with a Cobalt Long Line Focus X-ray tube using  $\text{K}\alpha$  radiation operating at 40 kV and 30 mA. Patterns were collected between 3 and 120°  $2\theta$  with a 0.02°  $2\theta$  step size and a scan rate of 0.6°  $2\theta$  per minute. Data were interpreted using a combination of X-plot for Windows (Version 1.34) and PCPDFWIN database (Version 2.02). QXRD results were obtained from diffraction patterns using Topas® version 3.0 from Bruker Advanced X-ray Solutions, employing the fundamental parameters approach to Rietveld analysis.

Replicate samples of ~5 mm granules, hand picked from ore and leach residues, were mounted in epoxy and the hardened blocks cut back using a diamond cutting wheel to expose the centres of the sample grains. The mineralogy of particles was inferred from data obtained using the QEMSCAN® advanced mineral analysis system. The particles were

examined using the Field Scan method, involving spot analyses over the surface of the block, collection of the resultant X-ray spectra and comparison with a spectral data base.

### **3. Results and Discussion**

Five inoculated columns, one non-inoculated column and two 'sterile' columns were studied to establish the leaching behaviour of the ore and to corroborate and/or interpret the results obtained from the test heap (Table 1). Column bioleaching tests generated typical nickel recovery curves, which are discussed briefly. However, copper recovery curves were atypical and unpredictable. Most insights on copper behaviour were obtained from the detailed ore and leached residue mineralogy.

#### *3.1. Nickel extraction*

In respect of nickel extraction (Figure 4), the main point to note is that all the columns operated in recovery mode whether deliberately inoculated (C1-C3, C5-C6), colonised by indigenous organisms or contaminant organisms transferred from columns in close proximity (C4) or sterilised through the addition of sodium benzoate to the leach solution (C7-C8). Inoculation during acid agglomeration may have been detrimental to bacterial growth or may just represent one of the extremes of variability experienced in these tests (Figure 4, compare C1 and C2).

Acid-agglomeration tended to favour nickel extraction initially compared with water-agglomeration (Figure 4, compare C2 and C3/C4) but did not ultimately control overall recovery. Rapid nickel recovery in 'sterile' columns (Figure 4, C7, C8) was indicative of the reactivity of pyrrhotite and, to a lesser degree, pentlandite with acid; both leach curves exhibited strong curvature subsequently. While aeration did not seem to be a key parameter early in the leach, it was required, together with bacteria, to sustain the rates of nickel recovery later in the leach. The pronounced delay in nickel extraction for C6 compared with C5 was accompanied by a similar delay in iron release; reservoir solutions contained less than 15 mg Fe/L in the 0-15 day period. This is indicative of poor pyrrhotite dissolution in C6 but is otherwise inexplicable.

The variety of leach curves exhibited here was previously experienced for the bioleaching of pentlandite concentrate and ore (unpublished data) and might be partly due



to the distribution of nickel between the reactive pyrrhotite and less reactive gangue and pentlandite phases in the ore (discussed in section 3.3). It should be remembered that leach curves such as those presented are the net result of many contributing and perhaps competing reactions.

The colonisation of the non-inoculated column C4 by a microbial population derived from the ore or microbial contaminants from nearby columns in the laboratory was clearly indicated by the slow increase in ferrous ion concentrations from 5 mg/L to 2300 mg/L (day 12) followed by a decrease to <5 mg/L by day 20 (Figure 5). Ferrous ion concentrations were generally low thereafter but exhibited intermittent excursions to high concentrations. This secondary microbial population, presumably distributed through the ore bed, would have contributed to the column bacterial population in each column and diminished the overall importance of the mode of inoculation in the comparative tests. Secondary inoculation of ores by indigenous or contaminant organisms also diminishes the value of using data from uninoculated 'control' columns to estimate the degree of bio-enhancement of metal extraction during bioleaching and highlights the need to monitor the presence of microbial cells in column effluents and reservoir solutions..

The much lower nickel extraction obtained in the columns (Figure 4) compared with the columns and test heap (Figure 3) could be due, in part, to the higher acidity of the pond water used to irrigate the test heap (pH 1.4-1.8) compared with the feed to the columns (pH 1.8-2.1). In the heap, the solution pH remained low enough to retain ferric ions in solution. In the columns, the pH rose to pH >2, a condition which allowed ferric ions to contribute to the formation of insoluble iron(III) compounds.

### 3.2. *Copper extraction*

In respect of copper extraction, only four of the columns operated in 'recovery mode' with virtually no copper extraction found in the other four (Figure 6). As was noted for nickel, inoculation of the ore during acid agglomeration might have been detrimental to the microbial population (Figure 6A, compare C1 and C2) and colonisation of indigenous or contaminant organisms rendered the non-inoculated column as efficient as those which were deliberately inoculated (Figure 6A, compare C4 and C2/C3).

For those columns where copper was extracted, initial copper release was slow compared with nickel. This is partly a consequence of both the well-known lack of

reactivity of chalcopyrite compared with pyrrhotite and pentlandite and of the chalcopyrite distribution in the ore (section 3.3). However, the slow start, reminiscent of the delay experienced in the test heap, could also be a consequence of pyrrhotite reactivity. [Kandemir \(1985\)](#) reported the odour of hydrogen sulfide prior to bacterial inoculation during the leaching of pyrrhotite in sulfuric acid, as did [Ahonen and Tuovinen \(1994\)](#) when leaching a pyrrhotite-rich chalcopyrite ore, again prior to bacterial inoculation. Pyrrhotite is known to dissolve in acid (Equation 1) with the release of hydrogen sulfide. Cupric ions may react with hydrogen sulfide in acidic media or directly with the pyrrhotite surface to form covellite (Equations 2 and 3). [Holmström et al. \(1999\)](#) reported that covellite existed both as discrete grains and as a precipitate, and copper ions adsorbed on pyrrhotite surfaces in chalcopyrite tailings. Note that in the same study, no secondary nickel enrichment zone or secondary minerals containing nickel were found.



Total iron concentrations in column discharge solutions ranged from about 100 mg/L initially to about 2,500 mg/L after 150 days. Ferrous ion concentrations were generally only 1% of the total soluble iron in inoculated columns, indicating that iron oxidising bacteria were active.

The sensitivity of copper recovery to ferric ion concentration is illustrated using data from the non-inoculated column C4 which subsequently became colonised (Figure 7). Colonisation (apparent at day 15) resulted in rapid biooxidation of ferrous ion to ferric ion (Figure 5) while at the same time, iron concentrations continued to increase as a result of pyrrhotite oxidation. Nickel solubilisation followed the trend for total iron regardless of iron oxidation state, but ferric ion was clearly required for copper solubilisation. In the aerated, inoculated columns, where ferric ion predominated from the start, copper release began immediately (Figure 7, broken line).

The poor recovery of copper in C5 (Figure 6B) compared with C2 (Figure 6A), cannot be explained from experimental data or observations made during column management. These columns were set up and operated similarly for the first 80 days, after which the air flow was shut off in C5. The redox potentials of the effluent solutions for both C2 and C5

rose to and remained at >650 mV vs Ag/AgCl, indicative of ferrous ion biooxidation, and the total iron concentrations rose to >2000 mg/L and >3000 mg/L, respectively.

Effluent redox potentials for the inoculated column C6 (Figure 6B) operated without aeration remained below 500 mV vs Ag/AgCl for most of the leach, indicative of greatly reduced bacterial growth and activity. The effluents from the two 'sterile' columns, C7 (aerated) and C8 (unaerated) both had redox potentials <400 mV vs Ag/AgCl (Figure 6B), indicative of abiotic operation. This was corroborated by both C7 and C8 having up to 7 g/L iron as ferrous ion in their effluents, a solution chemistry parameter that distinguished these columns from the others. In summary, it was concluded that the absence of sufficient ferric ions to oxidise the available sulfide minerals, particularly chalcopyrite, contributed to an environment in which copper-immobilisation reactions predominated over copper-release reactions.

Iron chemistry is inextricably bound to acid consumption because iron(III) insoluble oxides, hydroxides and/or hydroxysulfates may form at pH >2 within the ore bed, thus disproportionately depleting the solution of ferric ions. An estimate of iron(III) precipitation can be gained by comparing the maximum iron concentrations in the reservoir solutions for aerated inoculated columns (about 3000 mg/L) with those for the two sterile columns (about 7000 mg/L).

Pyrrhotite-rich ores are well known for their acid consuming properties. It is not surprising, therefore, that the pH values of the column discharge solutions were consistently higher than those of the feed (pH 1.8-2.1) by about 0.3 pH units. A relatively stable pH in the range pH 2 - 2.5 was reached once the initial (~5 days), strongly-acid-consuming phase of the leach was completed. During that initial phase, pH 3-4 was recorded for all discharge solutions. The ore continued to consume acid throughout the bioleach with acid additions to the reservoir being required on a daily basis to maintain the selected leach conditions. The addition rate was estimated to be about 0.4 kg/t ore per day. The extent to which the rising pH, which occurred during the passage of the leachate through the ore bed, had a direct impact on copper recovery could not be determined from the data. However, following the initial, strongly acid-consuming phase, the pH rises were near equivalent across the columns and, as such, should have a minimal contribution to the observed differences in copper recoveries.

### 3.3. Ore mineralogy and sulfide distribution

Quantitative X-ray diffraction analysis of the ore used in the column tests revealed that the main non-sulfide phases were augite (48%), amphibole (actinolite with magnesiohornblende - 24%) and chlorite (10%), with minor phases quartz and albite. The sulfide minerals were pyrrhotite (11%), chalcopyrite (2-4%), and pentlandite (1-2%).

For the purpose of determining mineral associations and mineral liberation of the sulfides using QEMScan (inferred mineralogy, Figure 8), the augite, magnesiohornblende and actinolite were grouped as a 'silicate matrix' and together comprised about 70% of the ore. These silicates were grouped because the similarity in their formulae made it difficult to distinguish between them using SEM-based elemental analysis.

Mineral association analysis indicated that pyrrhotite was 50% associated with the 'silicate matrix' and 20% associated with chlorite in the ore, with about 2% exposed on particle surfaces, the last representing about 8% of the total exposed particle surface area. The pyrrhotite contained within it about 8,500 mg Ni/kg and had an average formula  $\text{Fe}_{0.78}\text{Ni}_{0.02}\text{S}$ , estimated from spot elemental analyses using SEM. It has previously been reported that pyrrhotite may contain up to 7.47% Ni but the most common range is 50-500 mg Ni/kg (Fleischer, 1955) due to pentlandite exsolution. It is also worth noting that the chlorite phase contained about 1,700 mg Ni/kg and had an average formula  $(\text{Mg}_{2.24}\text{Fe}_{1.42}\text{Mn}_{0.03}\text{Cr}_{0.03}\text{Ni}_{0.03}\text{Al}_{1.1})(\text{AlSi}_3)\text{O}_{10}(\text{OH})_6$ .

The pentlandite had an approximate formula of  $\text{Fe}_{3.8}\text{Ni}_{4.5}\text{S}_8$ . Pentlandite grains, the majority about 40  $\mu\text{m}$  diameter, were mainly associated with pyrrhotite (25%). About 40% by mass of the pentlandite occurred as discrete encapsulated grains within the silicate matrix. Only 20% by mass comprised pentlandite grains >100  $\mu\text{m}$  diameter and about 50% of these had small surface exposure. About 4% of the pentlandite was associated directly with chalcopyrite. Overall, mineral liberation analysis indicated that only about 1-1.5% of the pentlandite grains had surface exposure on the ore particles.

Chalcopyrite grains, average formula  $\text{Cu}_{0.9}\text{Fe}_{0.98}\text{S}_2$ , were mainly associated with chlorite (20%) and the silicate matrix (about 65%) with only about 7% association with pyrrhotite and 2% association with pentlandite. Chalcopyrite occurred as both finely disseminated grains (<50  $\mu\text{m}$ ) in the silicate matrix and as larger chalcopyrite grains, up to 300  $\mu\text{m}$ . Liberation analysis indicated that chalcopyrite grain boundaries were <1% exposed at the surface, which represents about 3% of total exposed particle surface area.

Efficient heap leaching requires a compromise between (i) crushing an ore sufficiently finely to expose the target minerals for extraction and (ii) creating a bed of competent particles through which a solution will percolate over a prolonged period. In preliminary column tests (not shown), crush size did not impact greatly on either nickel or copper extraction. This result was consistent with the sulfide grains being distributed throughout the silicate matrix with limited surface exposure. Their liberation and exposure to leachate would require such a fine crush size as to prevent permeability through a heap. The results of heavy liquid separations showed that a crush size -0.3 mm was required to achieve significant liberation of the sulfide minerals, illustrated using sulfur analyses of float-sinks fractions (Figure 9), from the gangue illustrated by magnesium. It was hypothesised that either silicate or pyrrhotite dissolution would be rate-limiting for copper and nickel extraction from this ore.

#### 3.4. *Leached residue mineralogy*

Examination of polished sections of ore particles using QEMScan offered insights into the leaching of specific minerals and the formation of reaction products (Figure 10). Identified reaction products included elemental sulfur, gypsum, jarosite and goethite, with trace amounts of römerite and melanterite.

Pyrrhotite was the most reactive of the sulfides, being replaced by significant amounts of sulfur in both aerated and unaerated columns (Figure 10). Transition zones of incomplete oxidation from pyrrhotite to sulfur are apparent as speckled zones in the particle map. Intermediates (or end products) might include goethite, hematite and/or jarosite as well as remnants of unreacted pyrrhotite. The results are consistent with those of [Ahonen and Tuovinen \(1994\)](#) who reported that elemental sulfur was a major component in leached residues of a complex pyrrhotite-rich sulfide ore.

The oxidative chemistry of pyrrhotite to form elemental sulfur varies depending upon the leaching conditions, specifically the presence of ferric ions, acid/oxygen, or water/oxygen ([Belzile et al., 2004 and references therein](#)) (Equations 4-6).

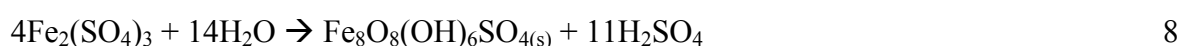


The presence of elemental sulfur in the residues implies that the sulfur oxidising organisms in the mixed culture could not oxidise sulfur as rapidly as it was produced. Sulfur oxidation rates for several acidophiles have been shown to be significantly slower in solutions of pH  $\geq 1.6-2$  (Plumb et al., 2008; Watling et al., 2008). Column discharge solutions ranged from pH 3.5-4 initially but varied between pH 1.8-2.5 for most of the leach, sufficiently high to cause slower rates of bacterial sulfur oxidation. Air limitation would also impact on sulfur biooxidation. In addition, examination of leached particles using QEMScan showed that the elemental sulfur was sometimes retained largely as a replacement of the pyrrhotite within the particle, possibly bounded by an 'iron-oxy-hydroxy-sulfate scale' on the particle surface (Figure 10) which may have restricted the access of sulfur-oxidising bacteria.

In contrast to pyrrhotite, many large and small grains of pentlandite and chalcopyrite remained unleached. Pentlandite grains are mainly associated with pyrrhotite (i.e., occurred in the vicinity of the sulfur reaction product) but were resistant to chemical attack. Many chalcopyrite grains are bounded by unreactive silicates, but those grains in the vicinity of the pyrrhotite/sulfur reaction zone and clearly exposed to acid and ferric ions also exhibited resistance to chemical attack. Preferential oxidation of pyrrhotite can be explained electrochemically. Natarajan (1988) reported rest potentials for the key sulfides in a copper-nickel ore under bioleaching conditions as chalcopyrite (+250-300 mV SCE) > pentlandite (+100-180 mV SCE) > pyrrhotite (+100-120 mV SCE) and noted that preferential oxidation of pyrrhotite would be expected, followed by selective leaching of nickel in preference to copper. He also noted that the secondary reaction of cupric ions with unreacted pyrrhotite (Equation 3) would influence copper recoveries. Limited evidence was obtained in the present column studies in respect of copper re-distribution as a function of depth, as might be expected if secondary copper ions were reacting with ore minerals, such as pyrrhotite. Chemical analysis of leached ore as a function of depth showed a small copper enrichment towards the base of the column (Table 2), whereas iron and nickel and gangue element contents were similar to those determined for the unleached head sample. The results were consistent with evidence of copper redistribution with depth obtained for test-heap samples using a selective cyanide leach to estimate 'non-chalcopyrite' copper content. However, in the present study, XRD analysis failed to detect copper species other than chalcopyrite in the leached column residues.

Examination of polished sections revealed extensive coating of particle surfaces by a relatively thick layer of iron-rich compounds (Figure 10, “Iron-Oxy-Hydroxy-Sulfates” phase). Crystalline phases in this layer, identified by XRD, were mainly goethite with less jarosite (predominantly hydronium jarosite) and small amounts of melanterite and römerite. In addition, XRD analysis, and mass-balances between mineral phases and chemical compositions indicated that the unidentified, poorly-crystalline phases in leach residues were comprised of iron-rich compounds such as schwertmannite and ferrihydrite. Some elemental sulfur was thought to be associated with the layer as there were sulfur-rich, oxygen-poor regions that reported as “pyrrhotite” – an inconsistency arising from the use of QEMSCAN inferred mineralogy to visualize the particles.

Goethite can be formed during pyrrhotite oxidation (Equation 6) or by hydrolysis of acidic ferric ion solutions (Equation 7). Its formation is promoted in solutions of pH >4 with relatively low sulfate concentrations, conditions which might have occurred near the base of the columns. In contrast, jarosite is precipitated from higher-concentration ferric sulfate solutions at pH 1.7-2.3 (Equation 3), conditions very similar to ideal bioleaching conditions and probably present at the tops of the columns. Schwertmannite is a poorly-crystalline, metastable phase that is a likely component of the unidentified iron-rich phases. It forms in ferric sulfate solutions low in monovalent cations and pH 2.8-4.5 (Equation 8), transforms slowly to goethite (Bigham et al., 1996; Carlson and Schwertmann, 2005) and is also a solid-phase precursor for jarosite formation in the presence of iron-oxidising acidophilic microorganisms (Wang et al., 2006). Conditions favouring the formation of goethite, jarosite or schwertmannite would have existed in both the aerated and unaerated columns during bioleaching. Ferrihydrite generally forms in less acidic conditions (pH >5) than were experienced in the bioleaching columns of this study but is difficult to identify using XRD in the presence of more crystalline compounds.



Two additional iron-rich phases, römerite ( $\text{FeSO}_4 \cdot \text{Fe}_2(\text{SO}_4)_3 \cdot 14\text{H}_2\text{O}$ ) and melanterite ( $\text{FeSO}_4 \cdot 7\text{H}_2\text{O}$ ) were detected in small amounts in the ore and the leached residues. They may be present as a result of the leaching conditions but are more likely artefacts of the residue rinsing and drying procedures applied prior to mineralogical analysis.

The iron-oxy-hydroxy-sulfate scale layer formed on many of the ore particles had a sufficient depth to act as a physical barrier to the transfer of reactants and reaction products between the bulk solution and mineral surfaces. For that period of leaching when the column discharge solution pH values were  $>\text{pH } 2$ , it may be assumed that ferric ion concentrations in the bulk solution would be depleted, thus limiting sulfide oxidation. In the case of chalcopyrite, the formation of a layer of insoluble iron-oxy-hydroxy-sulfate on the surface is an integral part of the oxidation mechanism and one of the suggested causes of “passivation” (Watling, 2006 and references therein). Stott et al. (2000) found that the layer formed on chalcopyrite concentrate under bioleaching conditions was a thick, coherent layer closely adhered to the chalcopyrite surface which could not be removed easily. In the present study, some chalcopyrite grains in the reaction zone were found to have such a layer, but other grains in close proximity did not. Yet the clean chalcopyrite surfaces showed little evidence of reaction, reflecting the mineral’s well-known intrinsically-slow leaching characteristics.

While the focus of this study was on copper reactions during bioleaching, the detailed mineralogical analysis also provided further insights on nickel extraction. Based on the quantitative mineralogy and the nickel contents of key phases, it was estimated that about 13% of the nickel in the ore was contained in the pyrrhotite with a further 3% in the chlorite. Pentlandite accounted for the remaining 84%. Initially it was hypothesized that the ~15% nickel recovery in the columns was achieved mainly through extensive pyrrhotite oxidation, partial chlorite oxidation but only minor pentlandite oxidation. However, it was found that nickel was incorporated into the mixed phases of the iron-oxy-hydroxy-sulfate scale (~2 wt% of scale), which covered some but not all of the remaining pentlandite grains specifically and the ore particles in general. Overall it was estimated that up to 45% of the initial nickel content in the ore had, at some point, been mobilised but that about two thirds of that was subsequently incorporated into the scale. Thus, it was concluded that a significant portion of the pentlandite must have been oxidised in addition to the pyrrhotite and chlorite. A preliminary investigation showed that about 50% of the nickel in the iron-oxy-hydroxy-sulfate scale could be recovered during a mild acid leach (pH 1.5-2.2), indicating that some of the nickel may have been incorporated in less reactive phases. The mobility of the nickel contained in the iron-hydroxysulfate scale is the subject of further investigation. The strategy of circulating the heap solutions through a barren rock pile (Figure 1) was employed at the Radio Hill test site to manage the formation of insoluble



iron compounds external to the test heap. It is possible that some of the nickel extracted during leaching in the primary heap was subsequently redeposited in the secondary iron-control heap.

## **5. Conclusions**

The key factors in copper recovery during the bioleaching of a low-grade, pyrrhotite-rich, copper-nickel ore are related to the reactivity of pyrrhotite in acidic solution and/or its reaction products.

The dominant acid-consuming reactions of the pyrrhotite resulted in column conditions under which ferric ions reacted rapidly to form insoluble iron-oxy-hydroxy-sulfate compounds which were deposited on particle surfaces as a layer of 'scale'. Both chalcopyrite and pentlandite oxidation may have been restricted by the consequent low concentrations of ferric ions. However, the effect would be more evident in the case of chalcopyrite because nickel would also be recovered from the acid leaching of pyrrhotite and chlorite and because pentlandite would be oxidised preferentially ahead of chalcopyrite. Thus, in contrast to nickel, where all columns exhibited positive leach curves, copper was only recovered from four of the eight columns studied.

While the iron-oxy-hydroxy-sulfate scale was of sufficient depth and integrity in some locations to have hindered the transfer of reactants and products from mineral surfaces to the bulk solution, there was significant evidence of reaction zones extending well into particles through the mediation of pyrrhotite dissolution. Thus, chalcopyrite liberation is thought not to be as significant a factor as proximity to pyrrhotite for enhanced leaching.

Some evidence was obtained of copper re-distribution from top to bottom of the columns during solution passage through the ore. While no additional copper species were detected in the leached column residues (XRD has a poor detection limit), it is nevertheless hypothesised that the main mechanism of copper immobilization following dissolution involved the reaction of cupric ions with hydrogen sulfide to form covellite. The reaction of pyrrhotite with acid to form hydrogen sulfide can become a dominant reaction under conditions of air limitation and also during abiotic leaching where ferric ions are not continually regenerated through bacterial activity.

The presence of elemental sulfur in leached residues indicated that sulfur biooxidation was either hindered physically — sulfur globules were retained at reaction sites, replacing

pyrrhotite, and were often bounded by the iron-oxy-hydroxy-sulfate scale layer — or that conditions prevailing in the column, such as high pH, were not conducive to sulfur biooxidation. Lack of aeration (oxygen, carbon dioxide) impacted on ferrous ion biooxidation and probably on sulfur biooxidation. Efficient sulfur and iron biooxidation could have countered the acid consumed by pyrrhotite dissolution and maintained a sufficient ferric ion concentration to effect greater chalcopyrite oxidation.

Finally, significant nickel was incorporated into the iron-oxy-hydroxy-sulfate scale, indicating greater pentlandite oxidation than was estimated initially from the column data. It is possible that nickel immobilization through incorporation into iron-oxy-hydroxy-sulfate precipitates in the secondary, iron-control heap could have occurred at the Radio Hill test heap, diminishing overall nickel recovery.

Following on from the data described in this paper, subsequent studies will be focused on the impact of aeration and solution pH on abiotic leaching of the ore and on the reactions and reaction products of copper interaction with pyrrhotite and pyrite.

### **Acknowledgements**

M. Maley is appreciative of financial support from Curtin University of Technology through a Curtin University Postgraduate Scholarship and for part funding from Titan Resources NL. Thanks are extended to Titan Resources NL for a description of the problem and for supplying the ore used in this study. We also thank B. Benvie and P. Austin for their advice concerning mineralogical analysis of the ore and column residues. The financial support of the Australian Government through the AJ Parker Cooperative Research Centre for Integrated Hydrometallurgy Solutions is gratefully acknowledged.

### **References**

- Ahonen, L., Tuovinen, O.H., 1994. Solid-phase alteration and iron transformation in column leaching of a complex sulphide ore. *In*: Alpers, C.N., Blowes, D.W. (Eds.), *Environmental Geochemistry of Sulphide Oxidation*, American Chemical Society, Washington, DC, pp 79-89.
- Belzile, N., Chen, Y.W., Cai, M.F., Li, Y.R., 2004. A review on pyrrhotite oxidation. *Journal of Geochemical Exploration* 84, 65-76.

- Bigham, J.M., Schwertmann, U., Traina, S.J., Winland, R.L., Wolf, M., 1996. Schwertmannite and the chemical modeling of iron in acid sulfate waters. *Geochimica et Cosmochimica Acta* 60, 2111-2121.
- Carlson, L., Schwertmann, U., 2005. The pH-dependent transformation of schwertmannite to goethite at 25 °C. *Clay Minerals* 40, 63-66.
- du Plessis, C., Barnard, P., Naldrett, K., de Kock, S.H., 2001. Development of respirometry methods to assess the microbial activity of thermophilic bioleaching archaea. *Journal of Microbiological Methods* 47, 189-198.
- Fleischer, M., 1955. Minor elements in some sulfide minerals. *Economic Geology* 50<sup>th</sup> Anniversary Volume pp 970-1024.
- Hiroyoshi, N., Miki, H., Hirajima, T., Tsunekawa, M., 2001. Enhancement of chalcopyrite leaching by ferrous ions in acidic ferric sulfate solutions. *Hydrometallurgy* 60, 185-197.
- Holmström, H., Ljungberg, L., Ekström, M., Öhlander, B., 1999. Secondary copper enrichment in tailings at the Laver Mine, Northern Sweden. *Environmental Geology* 38, 327-342.
- Hunter, C.J., 2001. A bacterially assisted heap leach. World Patent No. WO 01/44519 A1, 30p.
- Hunter, C.J., 2002. A method for the bacterially assisted heap leaching of chalcopyrite. World Patent No. WO 02/070757 A1 20p.
- Hunter, C.J., Williams, T.L., Purkiss, S.A.R., Chung, L.W.-C., Connors, E., Gilders, R.D., 2007. Bacterial oxidation of sulphide ores and concentrates. United States Patent No. US 7,189,527 B2, 8p.
- Kandemir, H., 1985. Fate of sulphide sulphur in bacterial oxidation of iron sulphide minerals. In Proceedings of the XV International Mineral Processing Congress (Cannes), Volume II, GEDIM, St.-Etienne, France, pp369-377.
- Lizama, H., 2001. Copper bioleaching behaviour in an aerated heap. *International Journal of Mineral Processing* 62, 257-269.
- Natarajan, K.A., 1988. Electrochemical aspects of bioleaching polysulfide minerals. *Minerals and Metallurgical Transactions* 5 (2), 61-65.

- Plumb, J.J., Muddle, R., Franzmann, P.D., 2008. Effect of pH on rates of iron and sulfur oxidation by bioleaching organisms. *Minerals Engineering* 21, 76-82.
- Puhakka, J.A., Kaksonen, A.H., Riekkola-Vanhanen, M., 2007. Heap leaching of black schist. *In* D.E. Rawlings, D.E., Johnson, D.B. (Eds.), *Biomining*, Springer, Berlin, pp139-151.
- Stott, M.B., Watling, H.R., Franzmann, P.D., Sutton, D.C., 2000. the role of iron-hydroxy precipitates in the passivation of chalcopyrite during bioleaching. *Minerals Engineering* 13, 1117-1127.
- Wang, H.M., Bigham, J.M., Tuovinen, O.H., 2006. Formation of schwertmannite and its transformation to jarosite in the presence of acidophilic iron-oxidizing microorganisms. *Materials Science & Engineering C-Biomimetic and Supramolecular Systems* 26, 588-592.
- Watling, H.R., 2006. The bioleaching of sulphide minerals with emphasis on copper sulphides – A review. *Hydrometallurgy*, 84, 81-108.
- Watling, H.R., 2008. The bioleaching of nickel-copper sulfides. *Hydrometallurgy*, 91, 70-88.
- Watling, H.R., Perrot, F.A., Shiers, D.W., 2008. Comparison of selected characteristics of *Sulfobacillus* species and review of their occurrence in acidic and bioleaching environments. *Hydrometallurgy* 93, 57-65.
- Wilson, A.D., 1960. The micro determination of ferrous iron in silicate minerals by a volumetric and colorimetric method. *Analyst* 85, 823-827.

Table 1. Column set up conditions

---

C1	Inoculated during acid agglomeration; aerated; irrigated
C2	Acid agglomerated; aerated; irrigated with inoculated pH 1.8 water
C3	Water agglomerated; aerated; irrigated with inoculated pH 1.8 water
C4	Water agglomerated; aerated; irrigated with pH 1.8 water (no bacteria added but colonisation occurred subsequently)
C5	Acid agglomerated; aeration ceased at 80 days; irrigated with inoculated pH 1.8 water
C6	Acid agglomerated; unaerated; irrigated with inoculated pH 1.8 water
C7	Acid agglomerated; aerated; irrigated with sterile pH 1.8 water (with Na benzoate)
C8	Acid agglomerated; unaerated; irrigated with sterile pH 1.8 water (with Na benzoate)

---

Table 2. Copper, nickel and iron (%) as a function of depth in leached column residues.

	Cu	Ni	Fe	Mg	Al	Si
Head	1.61	0.77	16.9	6.41	1.76	18.2
Top	1.30	0.52	13.0	6.51	1.49	18.3
Mid (~0.5 m)	1.56	0.52	13.5	6.43	1.45	18.4
Base (~1 m)	1.82	0.63	14.3	6.32	1.49	17.6

## Figure Captions

Figure 1. Simplified schematic of the test heap

Figure 2. Sulfide ore test-heap temperatures.

Figure 3. Element recovery from the tall column and test heap. The shading indicates the period when the heap was decommissioned, sampled and reconstructed.

Figure 4. Nickel extraction during bioleaching. ◆ C1; ◇ C2; ▲ C3; △ C4; ■ C5; □ C6; ● C7; ○ C8.

Figure 5. Colonisation of the non-inoculated column (C4) by iron-oxidising organisms and consequent decrease in ferrous ion concentrations (2<sup>nd</sup> axis, mg/L) in column discharge solutions. Equivalent data for an inoculated column (C2) are shown (open symbols).

Figure 6. Copper extraction (open symbols) and solution potential (closed symbols) during bioleaching. 6A. ◆ C1; ▲ C2; ■ C3; ● C4; 6B. ◆ C5; ▲ C6; ■ C7; ● C8; copper extraction in C7 and C8 was 0% within analytical error (not shown).

Figure 7. Copper, nickel and iron solubilisation with respect to iron oxidation state. Open symbols represent the period prior to column colonisation during which ferrous ion predominated in solution. ■ Fe; ● Ni; ▲ Cu; compared with ---- copper recovery in an aerated, inoculated column where iron was present as Fe(III).















Figure 8. QEMSCAN particle map illustrating the distribution of mineral phases in ore particles.  Sulfur  Pyrrhotite  Chalcopyrite  Pentlandite  Chlorite  Iron-Oxy-Hydroxy-Sulfates  Amphibole-Pyroxene “Silicate Matrix” [Edge-to-edge 5 mm]

Figure 9. Element contents of fractions after heavy liquid separations. Cu, Ni and Fe contents exhibited similar distributions to sulfur.

Figure 10. QEMSCAN particle map illustrating the distribution of mineral phases in leached ore particles.  Sulfur  Pyrrhotite  Chalcopyrite  Pentlandite  Iron-Oxy-Hydroxy-Sulfates  Amphibole-Pyroxene “Silicate Matrix”  Chlorite [Edge to edge 70 μm]. White spaces and cracks within the particle are ‘voids’ which may have been induced during sample polishing.



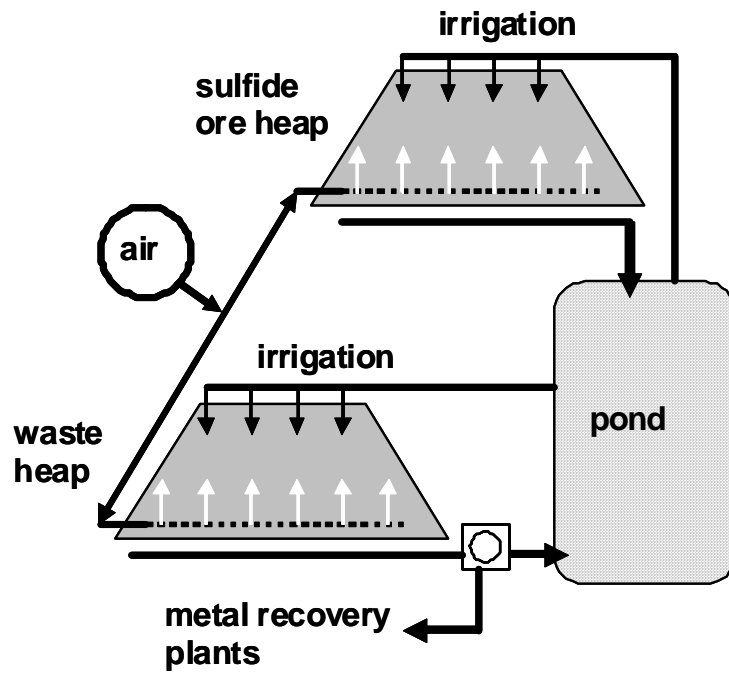


Figure 1. Simplified schematic of the test heap

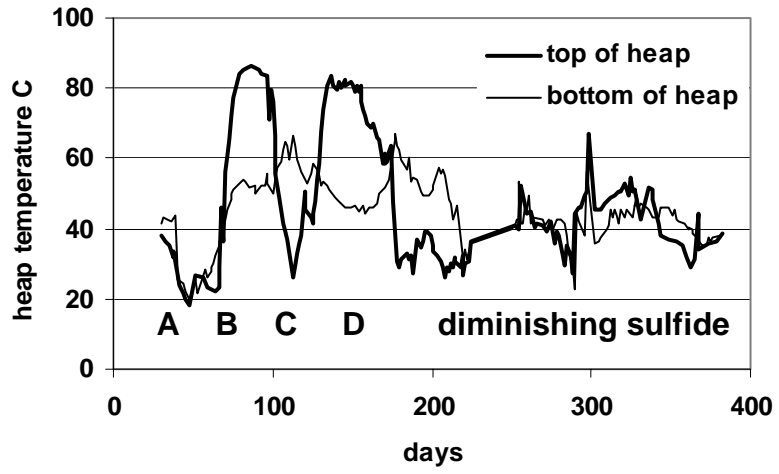


Figure 2. Sulfide ore test-heap temperatures.

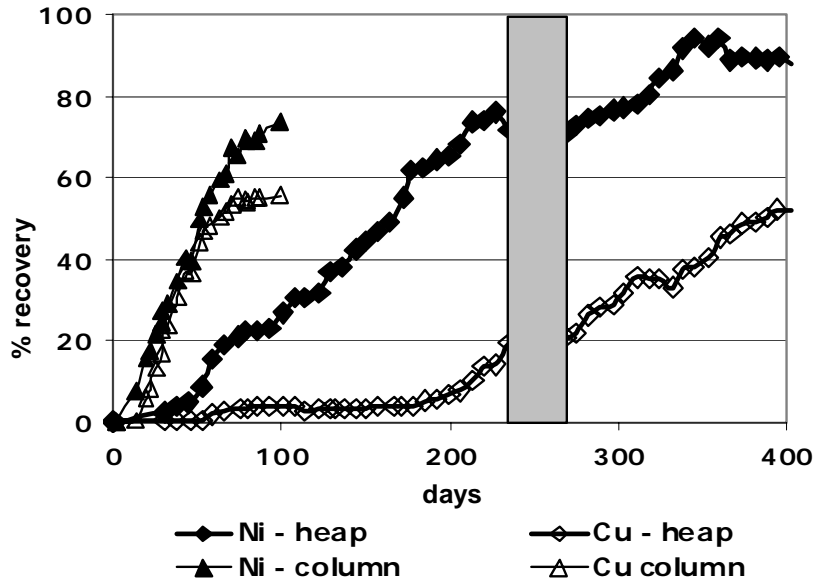


Figure 3. Element recovery from the tall column and test heap. The shading indicates the period when the heap was decommissioned, sampled and reconstructed.

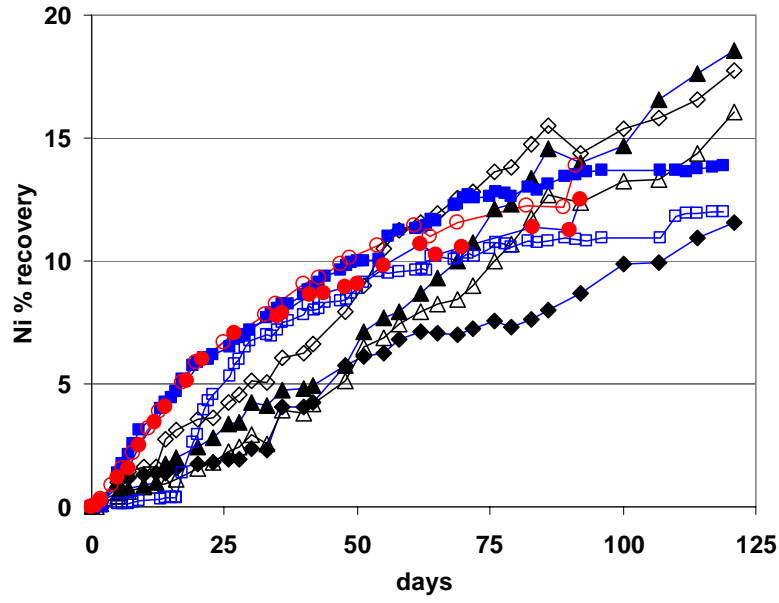


Figure 4. Nickel extraction during bioleaching. ◆ C1; ◇ C2; ▲ C3; △ C4; ■ C5; □ C6; ● C7; ○ C8.

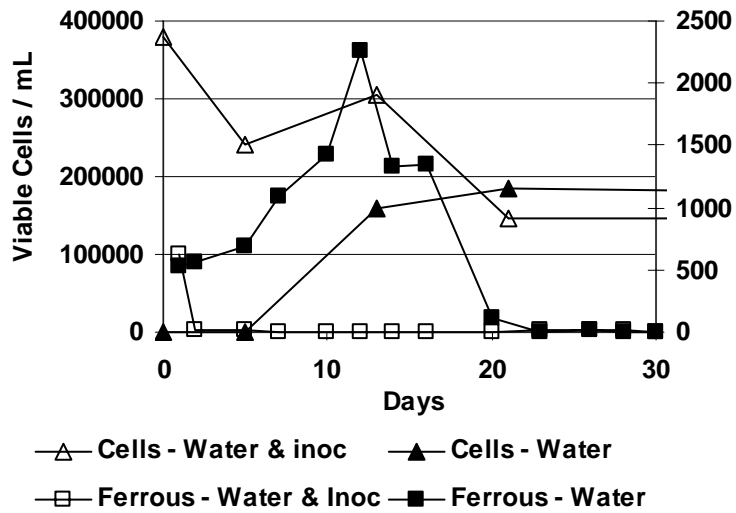


Figure 5. Colonisation of the non-inoculated column (C4) by iron-oxidising organisms and consequent decrease in ferrous ion concentrations (2<sup>nd</sup> axis, mg/L) in column discharge solutions. Equivalent data for an inoculated column (C2) are shown (open symbols).

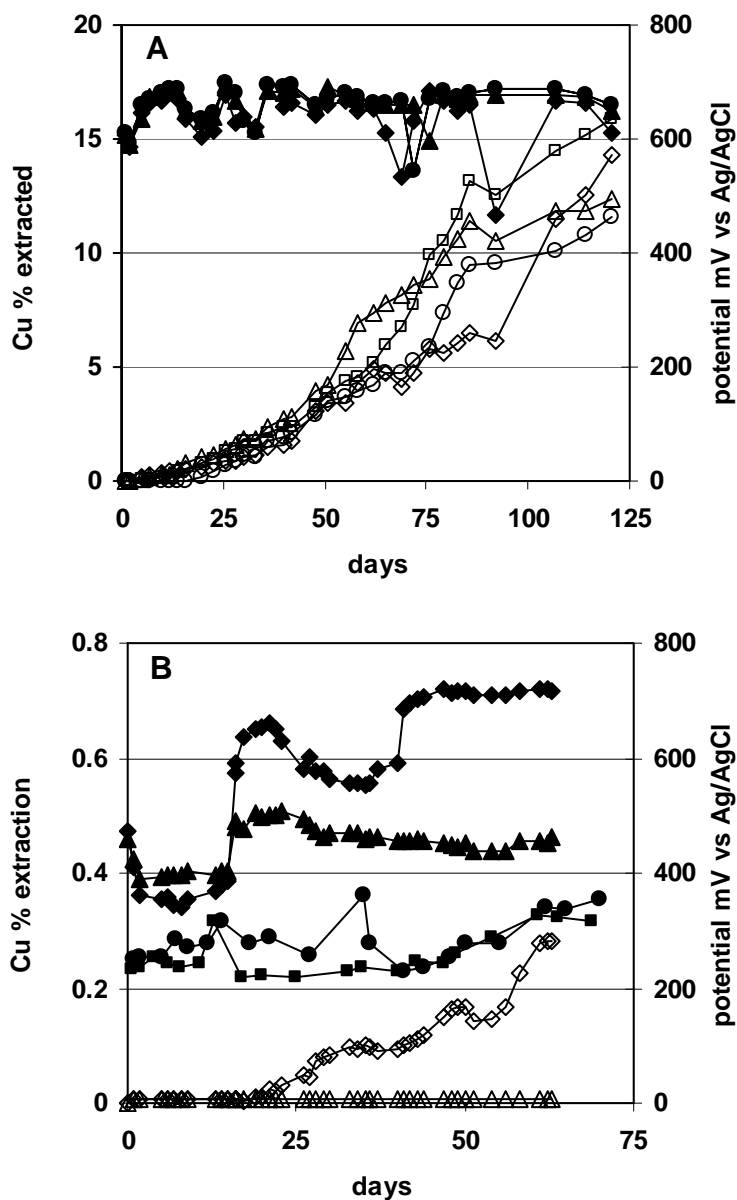


Figure 6. Copper extraction (open symbols) and solution potential (closed symbols) during bioleaching. 6A.  $\blacklozenge$  C1;  $\blacktriangle$  C2;  $\blacksquare$  C3;  $\bullet$  C4; 6B.  $\blacklozenge$  C5;  $\blacktriangle$  C6;  $\blacksquare$  C7;  $\bullet$  C8; copper extraction in C7 and C8 was 0% within analytical error (not shown).

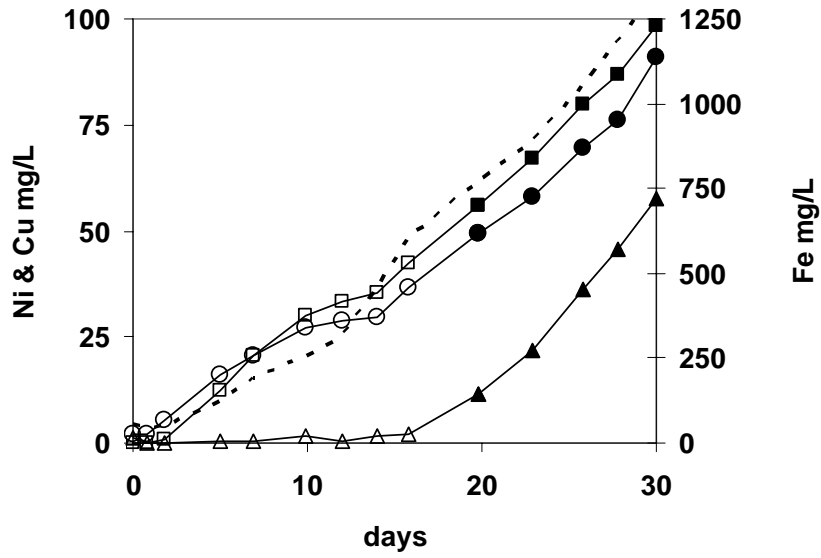


Figure 7. Copper, nickel and iron solubilisation with respect to iron oxidation state. Open symbols represent the period prior to column colonisation during which ferrous ion predominated in solution. ■ Fe; ● Ni; ▲ Cu; compared with ---- copper recovery in an aerated, inoculated column where iron was present as Fe(III).

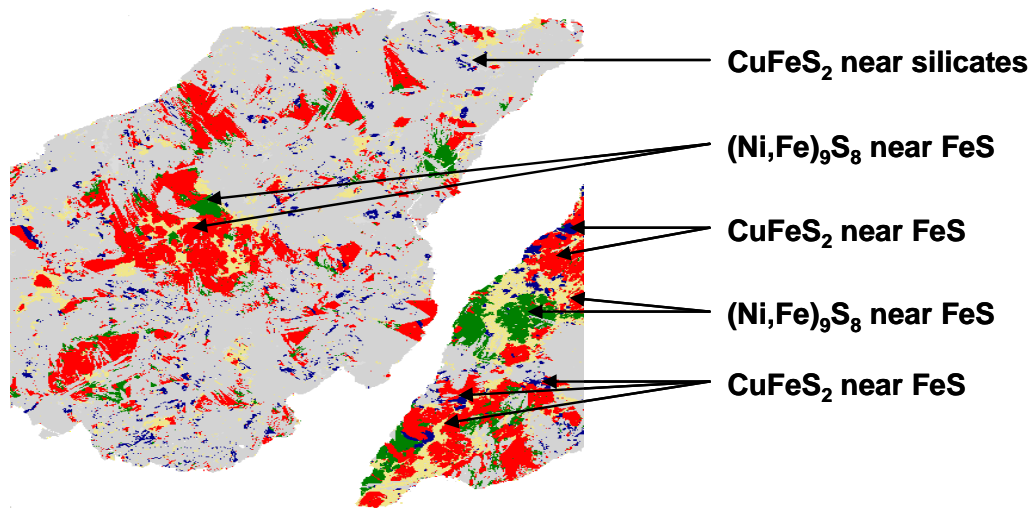


Figure 8. QEMSCAN particle map illustrating the distribution of mineral phases in ore particles. ■ Sulfur ■ Pyrrhotite ■ Chalcopyrite ■ Pentlandite ■ Chlorite ■ Iron-Oxy-Hydroxy-Sulfates ■ Amphibole-Pyroxene “Silicate Matrix” [Edge-to-edge 5 mm]



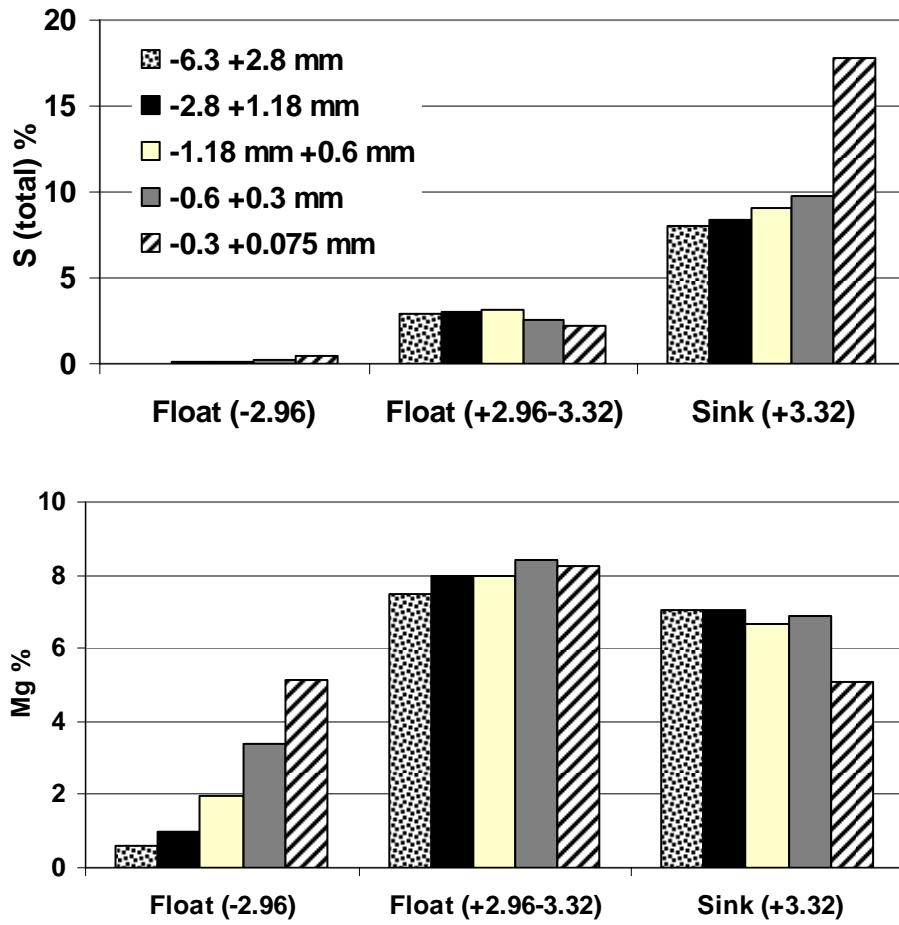


Figure 9. Element contents of fractions after heavy liquid separations. Cu, Ni and Fe contents exhibited similar distributions to sulfur.

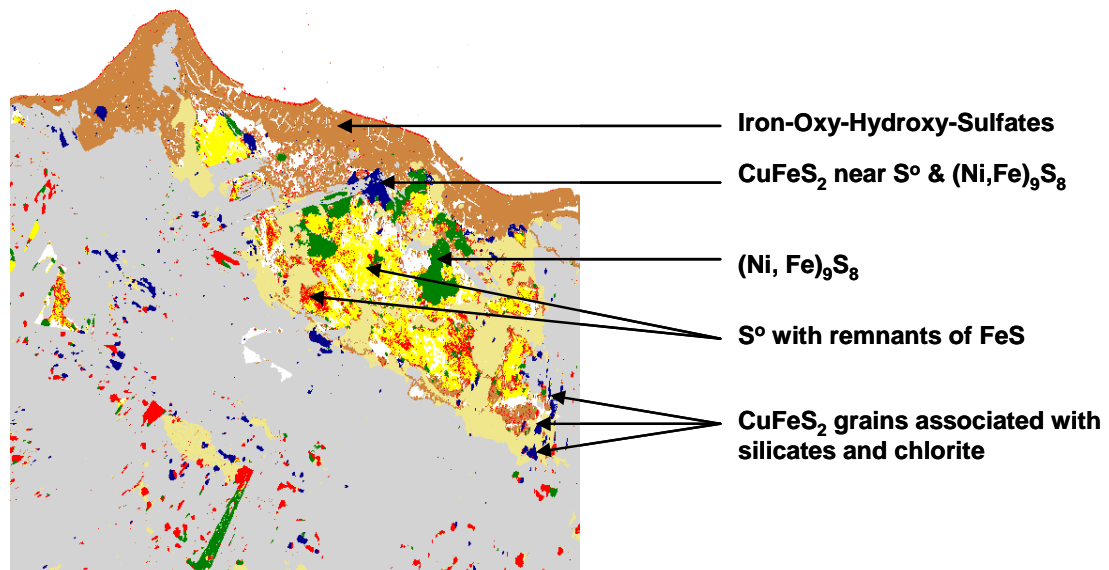


Figure 10. QEMSCAN particle map illustrating the distribution of mineral phases in leached ore particles. ■ Sulfur ■ Pyrrhotite ■ Chalcopyrite ■ Pentlandite ■ Iron-Oxy-Hydroxy-Sulfates ■ Amphibole-Pyroxene “Silicate Matrix” ■ Chlorite [Edge to edge 70 μm]. White spaces and cracks within the particle are ‘voids’ which may have been induced during sample polishing.